C.D. Thomson, J.R. Dennison, R.E. Davies, D.C. Ferguson, J.T. Galafaro and B.V. Vayner, "Investigation of the First Snapover of Positively Biased Conductors in a Plasma, "Paper AIAA-2000-0869, Proceedings of the 38th American Institute of Aeronautics and Astronautics Meeting on Aerospace Sciences, (Reno, NV, 2000). DOI: 10.2514/6.2000-869

AIAA-2000-0869

INVESTIGATION OF THE SNAPOVER OF POSITIVELY BIASED CONDUCTORS IN A PLASMA

C.D. Thomson, J.R. Dennison, and R.E. Davies
Utah State University, Logan, UT

B.V. Vayner, J.T. Galofaro, D.C. Ferguson and Win de Groot
John Glenn Research Center, Cleveland, OH

ABSTRACT

We describe a systematic experimental investigation of the phenomenon termed "snapover." In snapover, the current collected by a positively biased conductor, surrounded by a dielectric and immersed in a plasma, increases dramatically when the conductor potential is raised above some threshold value. The phenomenon is particularly relevant to the case of high-voltage solar arrays in Earth orbit. Our experiments examined the importance of conducting material, insulating material, size and shape of the conductor, sample history, biasing rate, and condition of the dielectric surface (contamination and smoothness) to the onset potential and current jump. In addition to a primary snapover occurring at approximately 200-350 volts positive bias, we observed numerous smaller current jumps from ~100 V to 200 V and much larger current increases at biases from +350 V to +600 V attributed to gas discharges. Both surface roughening and surface coatings were found to substantially inhibit snapover and gas discharge. Theoretical investigations and computer simulations have proposed that the fundamental physical process underlying snapover is secondary electron emission from the dielectric. Our attempts to confirm the importance of secondary electron emission in the mechanism responsible for snapover were not conclusive, but in general did not support previous simple interpretations of the SE model.

INTRODUCTION

In the past, satellite solar arrays have operated at voltages of less than 100 volts. However, as systems such as the International Space Station become larger and more complex, the power needed to run them has increased. To reduce transmission line mass and I^2R power losses, it becomes mandatory to design solar arrays which operate at higher voltages and lower currents.[1] At high operating voltages (several hundred volts) one has to consider possible detrimental interactions that can take place between the spacecraft and the space plasma environment. For instance, it is known that solar arrays biased negatively to several hundred volts exhibit destructive arcing.[2] Alternatively, arrays biased positively above a critical voltage (~100 volts) can undergo a phenomenon called "*snapover*." During snapover, the electron current collected by the exposed positively biased conducting interconnects (often termed a parasitic current, as it degrades the array's performance) exhibits a sharp increase at a critical bias voltage. This results in substantial power losses for the spacecraft. In addition, snapover can cause high negative counter potentials on other parts of the spacecraft that can lead to destructive arcing.[3] At times an optical glow accompanies the anomalously high current.[4,5] A number of researchers have addressed snapover theoretically and computationally; however, there has been little systematic experimental investigation done on the basic parameters of the phenomena.

MECHANISM

The majority of the theoretical formulations proposed over the past 15 years suggest that secondary electron

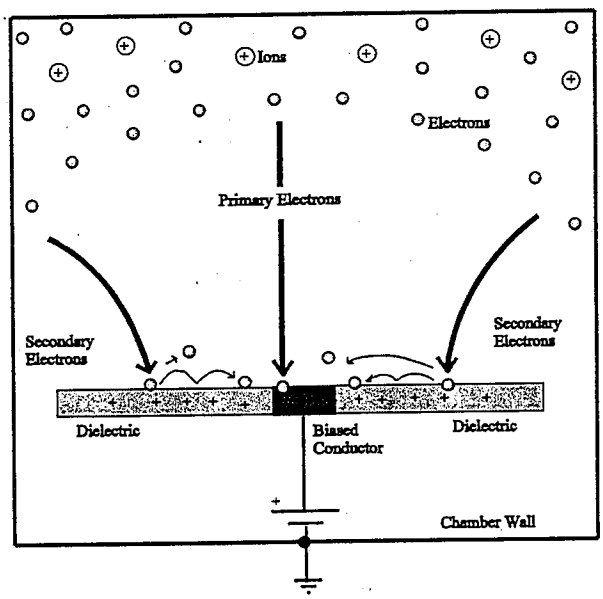

Figure 1. Proposed mechanism for snapover. Primary electrons are accelerated towards the positively biased conductor. Many bombard the surrounding insulator producing a shower of low energy secondary electrons. Many of these secondary electrons are collected by the conductor, causing the current to increase dramatically.

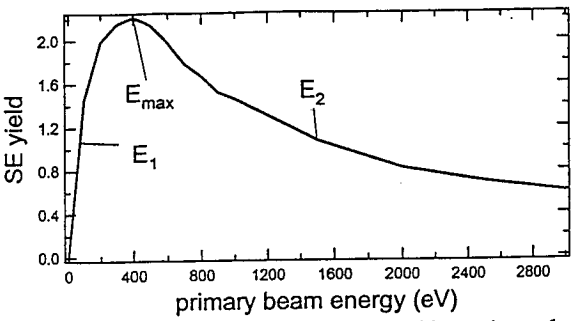

Figure 2. Curve of secondary electron yield vs primary beam energy for an untreated Teflon™ sample.[14] Other insulators have similar SE yield curves. The vertical axis represents the ratio of secondary electrons to primary electrons. The first crossover energy (E_1) occurs at the energy where the ratio rises to unity. Also shown are the energies where the ratio is a maximum (E_{max}) and where the ratio eventually falls back below unity (E_2).

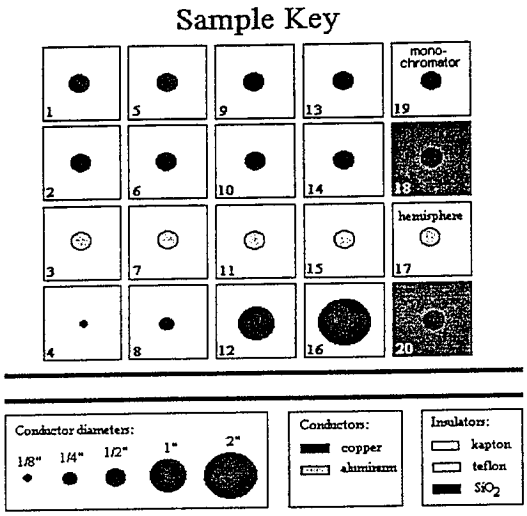

Figure 3. Key of conductor materials, shapes and sizes and insulating materials of the samples in the sample array.

emission--specifically, from the dielectric surrounding the positively biased conductor–is the fundamental physical process responsible for the anomalous currents underlying snapover.[6-8] Computer simulations of charged conductor/dielectric interfaces in the presence of secondary electrons (SE) and a plasma generally support this hypothesis.[9-13]

Secondary electron (SE) emission is the emission of electrons from a surface as a result of energetic electron bombardment. The vast majority of the emitted secondary electrons possess low energies (less than ~20 eV), and the total number of SE's produced per incident primary electron (PE) is a function of both material and incident energy, E_p.

In the most basic model of snapover the role of SE emission is generally believed to be as follows: (*i*) before snapover, the conductor/dielectric maintains equilibrium with the plasma primarily through a balance between incoming ion and electron currents regulated by an approximately hemispherical sheath above the positively biased conductor.[7,11,13] Ambient electrons enter the sheath by their own thermal energies, and once inside they accelerate radially inward towards the conductor. At this time, the dielectric remains at a near zero (slightly negative) potential;[9,13] (*ii*) Some of these electrons strike the dielectric immediately adjacent to the conductor with an energy equal to or somewhat less than the conductor bias (*i.e.,* for a conductor bias of +100 V, the electron kinetic energy upon striking the adjacent dielectric is E≤100 eV), producing secondary electrons from the dielectric. As the conductor bias is increased, so too is the energy with which the plasma electrons strike the edges of the dielectric, increasing the number of emitted SE's. Above some critical conductor bias the ratio of SE's to PE's (termed *SE yield, δ*) from the dielectric becomes greater than unity (see Figs. 1 and 2); (*iii*) Many of the SE's emitted from the dielectric are drawn in a "hopping" motion to the positively biased conductor, increasing the collected current.[6,7,10] Additionally, this leaves the portion of the dielectric near the conductor with a positive charge (slightly less positively charged than the conductor).[6,7,11,13]

Thus the dielectric itself begins to attract electrons from the plasma, with several important consequences. First, the number of SE's being produced by the now positively biased portion of the dielectric increases—the result of an increased flux of ambient electrons to the surface. Second, the sheath extends further into the plasma allowing greater interaction with ambient electrons.[4,10,11,13] Third, some of the ambient electrons attracted by the charged dielectric strike immediately adjacent, uncharged portions of the dielectric; these portions then begin to emit SE's and can become positively biased themselves, cascading the process until a large region of the dielectric surface is positively charged.[6,8,10,12] This entire process can lead to increased current collection by the conductor in two ways:

(a) Since, in general, the positive charge on the dielectric remains less than that on the conductor, most of the low energy SE's emerging from the dielectric surface see an electric field drawing them radially inward toward the conductor, where many are collected;[6,10,13]
(b) With a large region of the dielectric surface positively charged, the radius of the charge sheath surrounding the conductor/dielectric assembly increases—*i.e.*, more of the ambient plasma "sees" the biased conductor—exposing more ambient electrons to be captured by the positively biased conductor.[8-11,13]

Finally, within a very short time, a new equilibrium is established through a current balance between incoming electrons and outgoing secondaries which are collected by

Table 1. Secondary electron emission properties of materials used in this investigation. Listed yield and energy values for Teflon™, Kapton™, Al alloy 2024-T3, and OFHC copper were measured on as received samples that were cleaned by methods similar to those used in this investigation. In addition, listed SE yield values for Teflon™ and Kapton™ were measured using a pulsed beam method to reduce errors associated with dielectric charging. Alternate values and references for Teflon™ and Kapton™ are given in parentheses. The wide variation in insulator SE yield values was a crucial concern in testing the SE model of snapover.

Material	δ_{max}	$E_{p\,max}$ (eV)	E_1 (eV)	E_2 (eV)	References
Teflon™	2.2 (3)	396 (300)	69 (50)	1640 (1850)	14 (15)
Kapton™	1.6 (2.1)	222 (150)	75 (30)	651 (500)	14 (15)
SiO_2	2.1-4	300-450	40-45	2500	6, 16
Al alloy 2024-T3 (oxidized)	3.3	370	50	3670	17
Aluminum (clean)	0.70-0.75	350-400	--	--	18
OFHC Copper	1.14	790	370	1480	17
Microcrystalline graphite (Aerodag™)	0.45	500	--	--	19
MgO thin film	4-18	400-1500	30-80	> 4000	20, 21
Diffusion Pump Oil (Dow Corning 704)	1.8-2.0	140-150	≤75	90-100 eV	22

the conductor.[6,13]

This basic model describes many of the key features attributed to snapover; however, a more realistic charge gradient along the dielectric is required to better model the phenomena.[13] If this model is correct, the voltage required to initiate snapover (termed the onset voltage) should depend heavily on the SE properties of the dielectric material. Specifically, it should depend on the PE incident energy (and therefore the closely related conductor bias voltage) above which the insulator's SE yield is greater than unity–the so called "first crossover energy", E_1 (see Fig. 2).[6] Table 1 lists E_1 for the various materials used in this study, along with the maximum SE yield δ_{max}, the energy E_{max} at which δ_{max} occurs, and the second crossover energy E_2.

EXPERIMENT

As detailed as the theoretical explanations are, it is interesting that the previous ground based[4,7,8] and flight[23-25] experiments have been unable to confirm the detailed nature of snapover or the role played by SE emission. In response to the deficit of quantitative information, we designed a detailed systematic experimental research plan aimed at determining the fundamental parameters of the phenomenon.

An array of twenty samples of various predetermined materials, shapes, and sizes was constructed as shown in Fig. 3. Each sample was comprised of a 10 cm x 10 cm dielectric (either Teflon™, Teflon™ covered with Kapton™ tape, or SiO_2) with a conductor mounted in the center, flush with the front surface. Either OFHC Cu or Al alloy (Al 2024-T3) rods of 0.32 to 5.08 cm diameter conductors were used. Sample 17 was an Al alloy (Al 2017-T4) 1.27 cm diameter hemispherical conductor. The back side of the conductors were insulated to avoid snapover of the back side. The samples were cleaned with isopropyl alcohol each time the vacuum chamber was opened to remove accumulated contaminates.

The sample array was mounted vertically in the center of a 3 m high x 1.8 m diameter plasma chamber at the Plasma Interaction Facility (PIF) at NASA's Lewis Research Center (LeRC).[26] The chamber was pumped to a base pressures of ~10^{-6} Torr using three cold trapped oil diffusion pumps. Using Argon pressures of ~$1{\cdot}10^{-5}$ to $1{\cdot}10^{-4}$ Torr, plasmas were produced with standard Penning sources. A 2 cm diameter Langmuir probe determined typical plasma densities of ~$1{\cdot}10^{5}$ to $4{\cdot}10^{5}$ cm^{-3} and temperatures of ~1 to 3 eV

Starting at bias voltages of -100 V and typically ending at +600 V, a series of current vs conductor bias curves (typically 10 sweeps per run) were recorded for each conductor/dielectric pair. Although the step size and ramping rate were varied from 1V/s to 50 V/s on a number of samples, 10 V/s (5 V steps with 500 ms delays) were standard. Currents up to 10 mA were measured.

One additional sample was mounted in view of a spectrometer to analyze the glow that often accompanies the discharge phenomenon. The optical spectrum (350 nm to 600 nm) of a sample undergoing discharge was recorded.

Our experiments were designed to investigate the importance of:

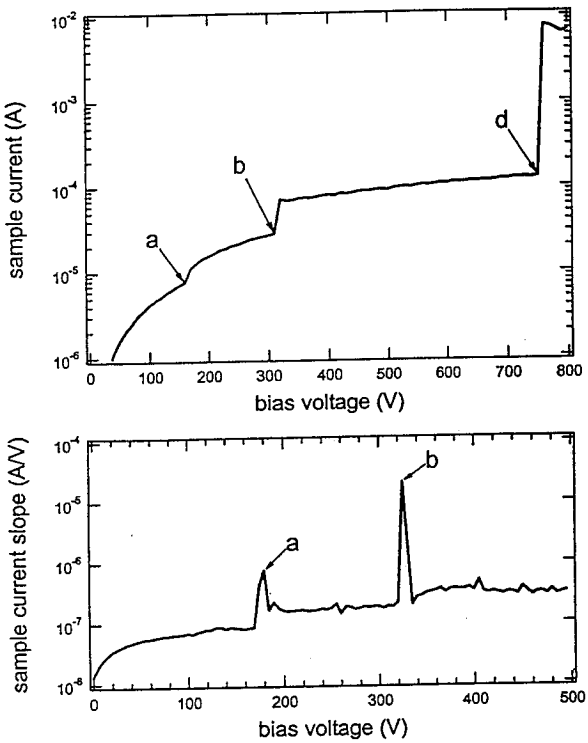

Figure 4. (Top) Current-voltage profile for a typical sample (½" Cu-Teflon™ sample #21). Profile exhibits current jumps attributed to (a) pre-snapover, (b) primary snapover and (d) Paschen discharge. (Bottom) Derivative plot of the snapover peaks. Note the logarithmic vertical axes in both graphs.

1. Cycling a given sample through multiple snapovers to study the effects (if any) due to sample surface alterations on the snapover onset voltage and current jump.
2. The effect of conductor biasing ramping rate (step size and time delay) on surrounding plasma dynamics and response rate and the snapover onset voltage or current jump.
3. The effect of surface contamination (such as diffusion pump oil) of both insulator and conductor surfaces on snapover occurrence, onset voltage and current jump. Even monolayer contaminant films have been shown to significantly modify SE emission.[27,31]
4. The effect of the ambient plasma density on plasma sheath formation and the snapover onset voltage or current jump. Charge available within the accessible plasma sheath should control the magnitude of the snapover current jump.
5. The type of insulating material surrounding a fixed conducting material–and particularly the insulator's first crossover energy–on the snapover onset voltage or current jump. Teflon™, Kapton™, and SiO_2 were chosen because of their relatively large range of the first crossover energies.
6. The type of conductor material (*e.g.*, Al and Cu) surrounded by a common insulator on the snapover onset voltage or current jump. Al and Cu were chosen because of there distinctly different SE emission characteristics.
7. The effect of the conductor size or shape (flat vs spherical) on plasma sheath formation and the snapover onset voltage or current jump. Hastings and Chang suggested that the snapover onset voltage should be significantly larger for a planar geometry than for a spherical one; hence, a hemispherical conductor (sample 17) was included for comparison.[6]
8. The effect of roughening a strip of the surrounding insulator to try to inhibit SE collection by the conductor and possibly prevent the snapover phenomenon. Previous experimental studies have reported inconsistent results for roughened surfaces.[7,28]
9. The effect of coating the surrounding insulator with colloidal microcrystalline graphite (Aerodag™) or MgO to try to modify the snapover phenomenon.
10. The optical spectra of the glow that sometimes accompanies the phenomenon. This can allow determination of the materials (*e.g.*, plasma, insulator, conductor, or outgassed species) involved in snapover or gas discharge.

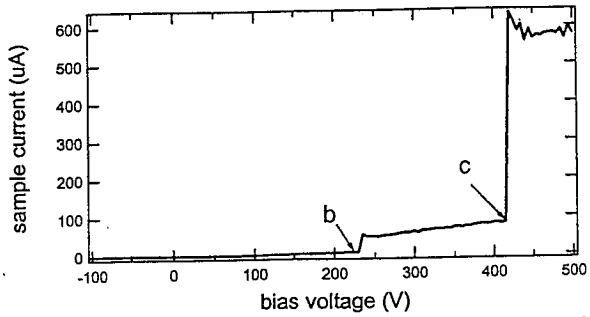

Figure 5. Current-voltage profile for a typical sample (½" Cu-Kapton™ sample # 1) showing current jumps attributed to (b) primary snapover and (c) gas discharge. Note the linear vertical axis and the characteristic hook shapes of the current jump profiles.

RESULTS AND DISCUSSION

A General Discussion of the Results

Examination of the I-V profile data revealed that most samples exhibited more than one current jump over the voltage range of approximately +100 V to +1000 V. After viewing the I-V curves for each sample (over 400 I-V curves in number), distinct patterns were observed that allowed categorization of the current jumps using the following criteria:

(i) Value of onset voltage;
(ii) Magnitude of current jump;
(iii) Comparison of trends in the I-V curves for consecutive measurements on a given sample;

Table 2. Primary snapover onset voltages and collection currents for untreated samples at relatively low to medium Argon pressures of 60-80 μTorr, electron number density of n_e=1-3·10^5 cm^{-3}, and electron temperature T_e=1-3 eV ramped at 10 V/s. First runs were excluded from the statistics. Standard deviations are shown in parenthesis.

Sample Type (Conductor Size-Dielectric)	Sample Number (see Fig. 3)	Onset Voltage (V)	Magnitude of Current Jump (μA)	Current Jump Ratio	No. of Runs	Snapover Occurrence Percentage
½" Cu-Teflon™	2	274 (38)	89 (66)	5 (2)	16	100%
½" Cu-Teflon™	6	278 (27)	12 (8)	1.6 (0.4)	6	100%
½" Al-Teflon™	3	219 (35)	18 (19)	3 (1)	11	100%
½" Al-Teflon™	11	--	--	--	3	0%
½" Cu-Kapton™	1	263 (27)	108 (63)	6 (4)	16	88%
½" Cu-Kapton™	5	224 (14)	51 (15)	3.0 (0.6	4	100%
½" Cu-SiO_2	18	259 (11)	94 (12)	10.6 (0.8)	9	100%
⅛" Cu-Teflon™	4	225 (54)	2. (2)	19 (23)	26	85%
¼" Cu-Teflon™	8	262 (36)	10 (11)	12 (13)	27	89%
1" Cu-Teflon™	12	198 (8)	68 (35)	3.0 (1.0)	8	100%
2" Cu-Teflon	16	226 (27)	215 (148)	1.9 (0.5)	21	100%
½" Hemispherical Al Alloy (Al 2017-T4)--Teflon™	17	271 (11)	140 (60)	5 (2)	9	100%
0.02 cm OD Cu on Ceramic (coax cable open end)	--	159 (5)	0.01 (0.00)	3.2 (0.2)	4	100%

(iv) Shape of the snapover curve (some current jumps were characterized by a hook shaped decline in the I-V curve immediately following the current jump as shown in Figs. 5 and 9).

By classifying each current jump using the above criteria, four major categories over the voltage range of 80 V to 1000 V were identified:

Preliminary Snapover: First, a small current jump (~ 1 μA to 10 μA for ½" conductors) could often be distinguished and occurred quite frequently over the voltage range of 150 V to 200 V, depending on the sample. Pre-snapover almost always occurred in conjunction with a larger snapover current jump as shown in Figure 4. Preliminary analysis of these current jumps indicated minimal response to ambient plasma conditions, suggesting that it may be a SE emission related phenomenon.

Primary Snapover: The second major current jumps (~ 10 μA to 100 μA for ½" conductors) occurred consistently in most runs at voltages ranging from 220 V to 350 V. These current jumps are the primary focus of this study. It was proposed that these current jumps were related to the SE emissions of the sample. Results are listed in Table 2 for the samples studied.

Gas Discharge: The third major category of current jumps (~ 0.1 mA to 5 mA for ½" conductors) appeared in a sporadic fashion from one run to the next and had onset voltages ranging anywhere from 350 V to 600 V. These larger current jumps were attributed to gas discharge in the near vicinity of the sample conductor. Similar current jumps of this magnitude and onset voltage range have been observed in previous experiments with similar interpretations.[7,8] Gas discharge may have resulted from ionization of sample out-gassing due to local heating or electron stimulated desorption. Results are listed in Table 3 for the samples studied.

Paschen Discharge: The fourth major category of current jumps (~2 mA to >10 mA for ½" conductors) also appeared intermittently with onset voltages ranging from ~500 V to 1000 V. These larger current jumps were attributed to breakdown of the background Argon gas.[29]

These four categories are identified on I-V curves in Figs. 4, 5, 7, 9 and 11 as (a) pre-snapover, (b) primary snapover, (c) gas discharge, and (d) Paschen discharge. In addition to these four major current jump categories, many smaller magnitude current jumps were observed throughout the voltage range of 80 V to 1000 V. Most of these jumps occurred irregularly and were attributed to contamination effects or as random gas discharges.

Although these four categories provided a general framework, ambiguities in classification did occur. For

Table 3. Gas discharge inception voltages and collection currents for untreated samples at relatively low to medium Argon pressures of 60-80 μTorr, electron number density of n_e=1-3·10^5 cm^{-3}, and electron temperature T_e=1-3 eV ramped at 10 V/s. First runs were excluded from the statistics. Standard deviations are shown in parenthesis.

Sample Type (Conductor Size-Dielectric)	Sample Number (see Fig. 3)	Gas Discharge Onset Voltage (V)	Magnitude of Current Jump (mA)	Current Jump Ratio	No. of Runs	Gas Discharge Occurrence Percentage
½" Cu-Teflon™	2	461 (38)	0.7 (0.5)	9 (6)	16	44%
½" Cu-Teflon™	6	458 (39)	1.1 (0.2)	24 (2)	6	33%
½" Al-Teflon™	3	386 (46)	0.4 (0.2)	14 (7)	11	73%
½" Al-Teflon™	11	323 (56)	0.27 (0.05)	25 (5)	3	100%
½" Cu-Kapton™	1	414 (44)	1.0 (0.4)	11 (4)	16	44%
½" Cu-Kapton™	5	457 (48)	1.5 (0.4)	12.1 (0.7)	4	75%
½" Cu-SiO_2	18	510 (60)	5.7 (0.7)	16 (15)	9	89%
⅛" Cu-Teflon™	4	454 (81)	0.3 (0.2)	101 (32)	26	23%
¼" Cu-Teflon™	8	393 (48)	0.2 (0.1)	38 (17)	18	61%
1" Cu-Teflon™	12	472 (28)	1.9 (0.4)	9.9 (2.1)	8	75%
2" Cu-Teflon	16	477 (86)	4.1 (3.5)	4.7 (3.7)	21	57%
½" Hemispherical Al Alloy (Al 2017-T4)--Teflon™	17	485	4.1	21	9	11%
0.02 cm OD Cu on Ceramic (coax cable open end)	--	--	--	--	4	0%

example, the onset voltage of the primary snapover and pre-snapover current jumps could "drift" from run to run and in some cases "fuse" together. Alternately, the primary snapover onset could drift to higher voltages from one run to the next (350 V to 400 V in some cases), and take on properties similar to gas discharge (large collection currents and the "hook" shaped current jump). It was not always clear which mechanism was occurring or whether both modes were occurring simultaneously, and if they were interrelated. Because of the occasional confusion involved in classification: (i) all major current jumps (>10 μA) below 350 V were categorized as primary snapover unless a clear distinction could be made with the preliminary snapover and (ii) any large magnitude current jumps occurring over ~350 V were identified as either gas discharge or Paschen discharge.

(1a) Snapover Behavior in First Ramping Cycles

The I-V curves resulting from the initial ramping cycle performed on each sample exhibited behavior which was not displayed in subsequent runs; hence these first runs were excluded from the sample statistics used to determine the importance of the other parameters explored in our investigation. The first run on a virgin sample produced many anomalous current jumps that were not repeatable. Two different types of current jumps, a low voltage snapover and a high voltage gas discharge, were noted to occur frequently for most samples. At background Argon pressures of 60-80 μTorr, irrespective of conductor or dielectric material type, initial ramping cycles exhibited an abnormal low voltage snapover at 122±22 V with a 75% occurrence rate and an initial gas discharge at an average voltage of 475±28 V with a 83% occurrence rate.

After this initial cycle, the surface of the sample seemed to change and more consistent current jump behavior was observed in subsequent cycles. The initial abnormal behavior of samples was attributed to liberation of materials such as oil and water initially adsorbed to the sample surface or trapped in the conductor/insulator junction. At high voltages and low pressures, either surface heating or electron-induced desorption allowed surface neutrals to escape, only to be quickly ionized by the high density of electrons near the dielectric surface. Electrons freed during the ionization were immediately drawn to the positive conductor creating the anomalous current jump.

(1b) The Effects of Multiple Runs on Snapover

The effects of multiple runs on a sample were studied

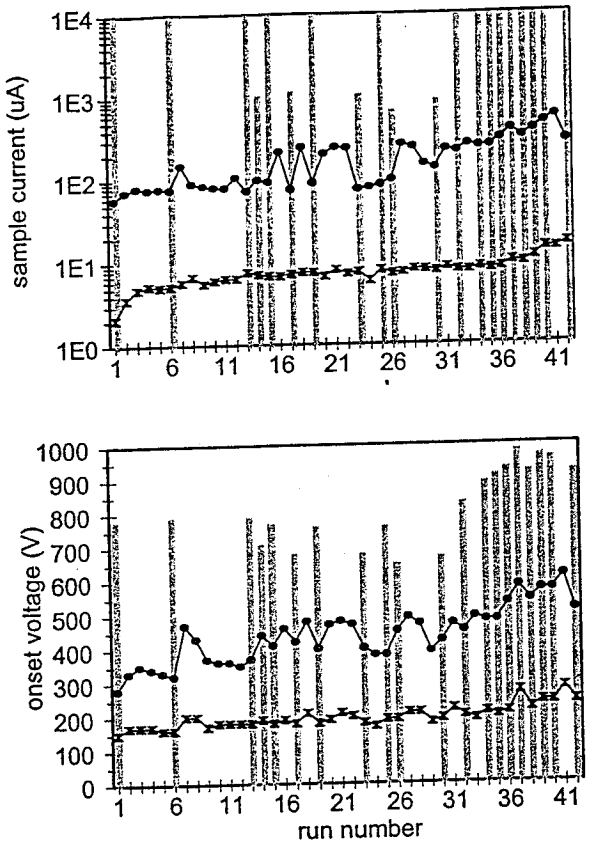

Figure 6. Response to high voltage discharge (either gas discharge or Paschen discharge) of sample current (top) and onset voltage (bottom) for primary snapover (x) and gas discharge(•). Vertical bars indicate the voltage and current magnitude, respectively, for the high voltage Paschen discharge that occurred during a given run for a ½" Cu-Teflon™ sample.

using a set of 43 consecutive runs on a ½" Cu-Teflon™ sample. These ramping cycles ran from 100 V to 800 V (1000 V for the last eight runs) at 10 V/s with background pressures of 210-230 μTorr. Two current jumps were observed for all 43 runs the first occurring from 196±27 V–attributed to primary snapover–and the second at 437±78 V–attributed to gas discharge. A very large current jump–attributed to Paschen discharge–occurred intermittently at 818±110 V.

The Paschen discharge seemed to affect the surface of the sample, and consequently the behavior of subsequent lower voltage current jumps. Figure 6 shows the response of the onset voltage and collection current of the primary snapover and gas discharge jumps to the Paschen discharge (bars) for consecutive ramping cycles. The primary snapover onset voltage and current jump magnitude were not significantly affected by the Paschen discharge for the first 34 runs after the initial cycle. However, the collection current and onset voltage of the gas discharge jump often increased substantially in cycles immediately following a

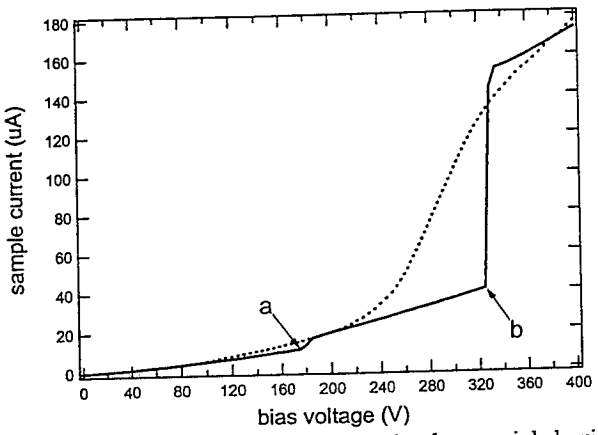

Figure 7. Current-voltage profile showing hysteresis behavior of a typical sample (½"Cu-Teflon™ sample # 2) for a full cycle of increasing (solid curve) and decreasing (dotted curve) voltages. Current jumps labeled (a) and (b) are attributed to pre-snapover and primary snapover, respectively.

Paschen discharge. For the last eight runs, the sample was ramped up to 1000 V to induce more frequent Paschen discharges. For these last seven runs the onset voltage and current collection of both the primary snapover and gas discharge steadily drifted to higher values.

This behavior suggests that the higher energy, more intense Paschen discharge jump modified the surface, perhaps through thermal- or electron-induced desorption or oxidation, and that the gas discharge jump was sensitive to the surface modifications while the snapover peak was less sensitive.

(1c) Hysteresis

As shown in Fig. 7, current jumps in the voltage range of 100 V to 700 V exhibited hysteresis. As a general rule, for a given ramping cycle the return I-V curve would fall rapidly with the major forward current jump, but then it would not respond as dramatically to any smaller lower voltage snapovers.

(2) Effects of Ramping Rate (Voltage Step and Time Delay) on Snapover Onset Voltage and Collection Current

The bias voltages reported in this study were measured between the sample and chamber ground. To compare the bias voltages to the SE emission energies of the materials investigated, the potential of the sample with respect to the plasma must be estimated. Three correction terms are considered: a quasi-static bias between the chamber and the far-field plasma adjacent the chamber walls; the response time for the plasma sheath in close proximity to the charged sample; and the response time between the plasma sheath and sample to the far-field plasma associated with the chamber geometry. The value of the plasma potential with respect to the chamber was determined by a Langmuir probe at

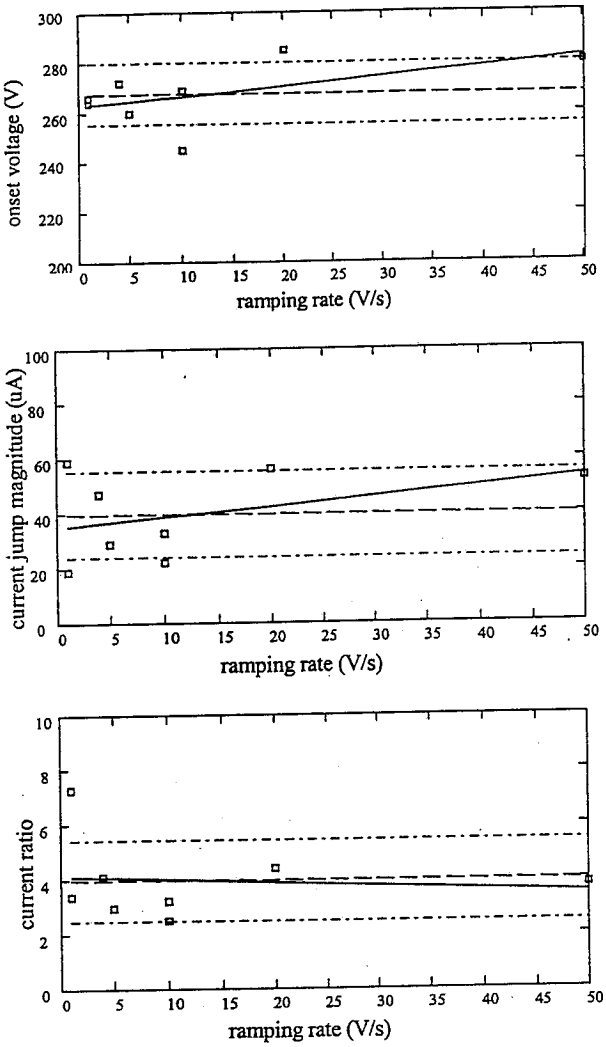

Figure 8. Effect of ramping rate on (a) onset voltage, (b) magnitude of current jump and (c) current jump ratio, respectively, for the primary snapover current jump of a typical sample (½" Cu-Teflon™ sample #2). Symbol shows data, while dashed and dash-dotted lines indicates the average value and limits of uncertainty to within ±σ, respectively. Solid lines are linear fits to the data. In each case, there is no statistically significant dependance on ramping rate.

the beginning of each series of cycles. Its value varied from -3 V to +25 V depending on the experiment. Because of the relatively high plasma density and resulting short Debye length (~2 cm), the response time for the plasma sheath adjacent to the sample is <1 ms; this caused no significant offset on time scales related to our ramping rate.[13]

Vayner *et al.* determined an upper bound of ~15 s for the response time between the plasma sheath and the far-field plasma by modeling the response of the system to an instantaneous 0 V to 500 V voltage step (50 V/s was the largest ramping rate used on any sample for the present study, although most data was taken at a ramping rate of 10 V/s).[29] Using 15 s as an upper limit of the response time, the analysis of Vayner *et al.* suggested that the plasma sheath to sample potential difference lagged behind the measured bias by ≤50 V. To verify this prediction, the current jump onset voltage response to ramping rate (voltage step and time delay) was measured for a ½" Cu-Teflon ™ sample at a pressures of 66 μTorr. Data shown in Fig.8 indicates that there is no statistically significant dependance of the primary snapover current jump onset voltage, current jump magnitude or current ratio on ramping rate. Figure 9 shows an increase of <15 V in the primary snapover onset voltage in three sequential cycles when the ramping rate was increased from 1 V/s to 50 V/s. Thus, the offset potential due to relaxation rate may be substantially less than suggested by Vayner *et al.* Further evidence of this conjecture came from stepping the sample bias by increments of 10 V, 25 V, and 100 V while manually recording collection current stabilization times. Of these, only voltage steps of 100 V produced relaxation times $\geq 10^{-1}$ s.

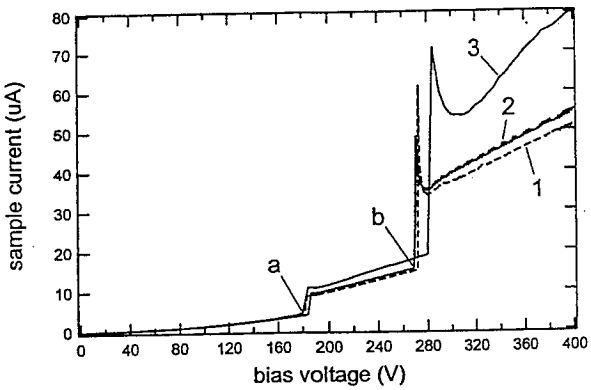

Figure 9. Sequential current-voltage profiles for a typical sample showing the effect of ramping rate for (1) 4 V/s, (2) 10 V/s and (3) 50 V/s. Current jumps at (a) and (b) are attributed to pre-snapover and primary snapover, respectively. Measurements were made on a ½" Cu-Teflon™ (sample #2) at a pressure of $7 \cdot 10^{-5}$ Torr.

Taken together, modeling indicates the measured bias may be between ~15 V and 50 V higher than the actual sample to plasma sheath potential, but direct measurements suggest a smaller voltage offset ≤15 V for 10 V/s ramping rates.

(3) Dependence on Surface Contamination

Surface contamination presented a serious limitation to our experiments. After approximately ten cycles, samples would develop a visible yellow ring around the conductor, identified as diffusion pump oil originating from the vacuum system of the plasma chamber. We estimated the deposition rate of diffusion pump oil as ~30

nm/cycle (approximately half the wavelength of visible light per ten cycles).[30] By contrast, the maximum escape depth of SE for diffusion pump oil is 2-3 nm.[22] Since SE emission of low energy electron is very surface sensitive, even monlayers of contamination can significantly affect emission.[27,31]

Therefore, the effects of chamber contamination on our data were undeniable. This impeached the verisimilitude of our studies of the dependence of snapover on sample materials, since in some ways all samples were effectively similar diffusion pump oil. SE emission properties of diffusion pump oil are listed in Table 1.

(4) Dependence on Plasma Parameters

The effects of plasma parameters are discussed in more detail in Vayner *et al.*[29] and are summarized here for the sake of completeness. The use of either Ar or Xe as the background gas had no discernable effects, except in the measured optical glow spectra discussed below. Increased background gas pressure or equivalently plasma density, did not effect the pre-snapover onset voltage or current jump magnitude, but may have had a small effect on the primary snapover onset voltage, and led to increased occurrence of Paschen discharges. No systematic study of the effect of plasma temperature was done.

(5) Dependence on Sample Dielectric Type

To determine the importance of sample dielectric and conductor [see *(6)* and *(7)* below] materials on snapover, multiple biasing cycles were performed at a constant ramping rate of 10 V/s under similar plasma conditions of 60-80 μTorr Argon pressure, electron number density of n_e=1-3*10^5 cm^{-3}, and electron temperature T_e=1-3 eV.

The measured primary snapover onset voltages for samples with ½" Cu conductors and different dielectrics (see samples 1, 2, 5, 6 and 18 in Table 2) are, in increasing order, Kapton™ (247±23 eV), SiO_2 (259±11 eV), and Teflon™ (275±34 eV). The measured gas discharge onset voltages (see Table 3) are, in increasing order, Kapton™ (433±50 eV), Teflon™ (460±33 eV), and SiO_2 (510±60 eV). In contrast, literature values of the first crossover (see Table 1), in increase order, are SiO_2 (40-45 eV)[16], Teflon™ (69 eV)[14], and Kapton™ (75 eV).[14]

These results suggest that measured primary snapover and gas discharge onset voltage were not dependant on the dielectric first crossover energy. Specifically:

(i) Measured variations in the primary snapover or gas discharge onset voltages were not statistically different form one another.

(ii) The order of increasing primary snapover or gas discharge onset voltage were not consistent with the order of first crossover energies. The values of crossover energies for insulators reported in the literature have large uncertainties, making it difficult to evaluate their effect on snapover in this manner.[14-16]

(iii) The primary snapover onset voltage values were ≥180 V higher than the first crossover energies of any of the dielectrics or of diffusion pump oil. Even after corrections for the offset voltages discussed in *(1b)*, the measured onset voltages were still more than 100 V above the first crossover energies.

Likewise (see Tables 2 and 3), variations due to dielectric material in the current jump magnitude and current jump ratio for both primary snapover and gas discharge were comparable to their uncertainties and showed no significant dependance on dielectric type. The sole exception was that the current jump ratio (before and after snapover) was higher for SiO_2.

A dependance on dielectric first crossover energy could not be conclusively ruled out due to poor statistics resulting from the inadequate number of samples tested. Also, the large uncertainty in the onset voltages may have been due to variations from run to run in the offset voltage [see *(1b)* above] surface contamination [see *(3)* above] effects. Finally, the extensive contamination of the samples by diffusion pump oil may have masked any dependence on dielectric SE emission properties.

(6) Dependence on Sample Conductor Type

Comparison of results in Tables 2 and 3 for ½" Cu-Teflon ™ samples (samples 2 and 6) with ½" Al-Teflon ™ samples (samples 3 and 11) suggest statistically significant differences due to conductor type. Aluminum conductor samples exhibited lower primary snapover and gas discharge onset voltages and current jump magnitudes than samples with copper conductors. Results for the current jump ratio are inconclusive.

Dependence of snapover or gas discharge current jumps with conductor type was not expected. These trends may reflect differences in the adsorption or removal of diffusion pump oil from the metals. For example, the Al had an insulating film of Al_2O_3 that may have led to surface charging and accumulation of the polarizable diffusion pump oil, while the oxide of Cu formed in a vacuum is conducting.[32] There may also have been differences in the surface roughness of the Al versus Cu conductors that could have affected SE emission and snapover directly [see *(9)* below] or affected adsorption/desorption of contaminants.

(7a) Dependence on Sample Conductor Size

The effects of conductor size on snapover and gas discharge current jumps were tested using five Cu-Teflon™ samples (samples 4, 8, 2 and 6, 12, and 16) with different conductor diameters (0.32 cm, 0.64 cm, 1.27 cm, 2.54 cm, 5.1 cm) respectively. Results are presented in Fig. 10. For both snapover and gas discharge no statistically significant correlation was found between the onset voltage and conductor diameter.

However, the current jump magnitudes and current jump ratios showed clear power law relationships to conductor diameter, $\Delta I \propto d^n$. The current jump magnitude

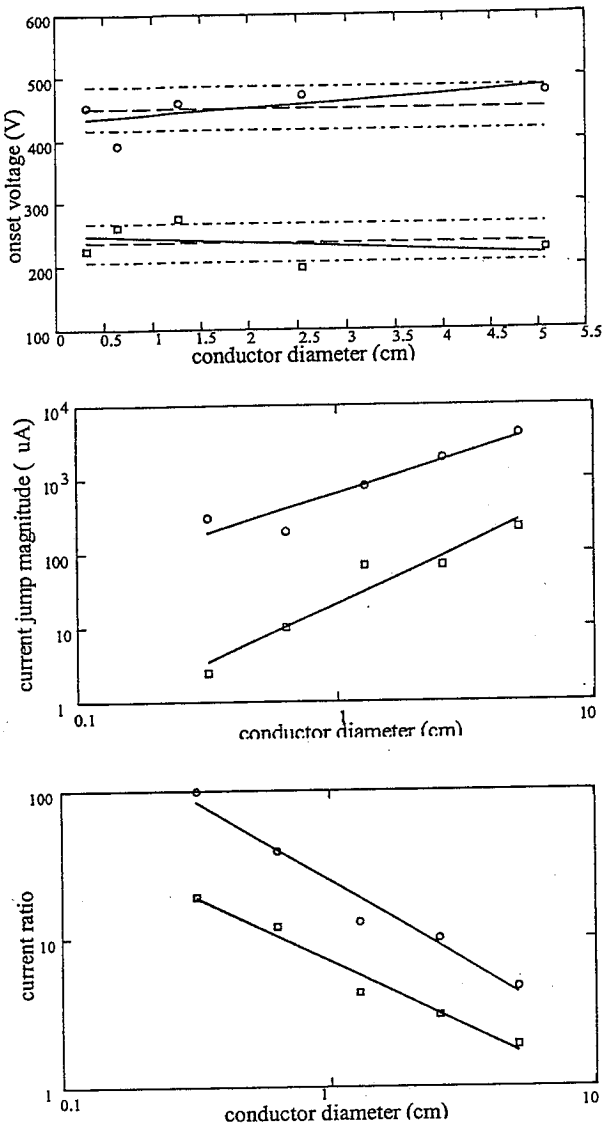

Figure 10. Effect of conductor size on (a) onset voltage, (b) magnitude of current jump and (c) current jump ratio, respectively, for the primary snapover current jump (•) and gas discharge (■) of Cu-Teflon™ samples. (a) Dashed and dash-dotted lines indicate the average values and limits of uncertainty to within ±σ, respectively. Solid lines are linear fits to the data.

was approximately linearly proportional to diameter or interface length (n=+1.6±0.3 for primary snapover and n=+1.1±0.2 for gas discharge). The current jump ratio was approximately inversely proportional to conductor diameter (n=-0.87±0.09 for primary snapover and n=-1.1±0.1 for gas discharge). For smaller conductor diameters, Stillwell et al. reported similar findings that collection currents increased continuously with increasing conductor diameter (with n<2) for voltages <1000 V.[7]

(7b) Dependence on Sample Conductor Shape

The effects of conductor shape on snapover and gas discharge current jumps were tested using a ½" diameter Al alloy hemisphere (sample 17) and ½" diameter Al alloy disks (samples 3 and 11). The onset voltage for the hemispherical conductor was 52 V higher for primary snapover and 99-162 V higher for the gas discharge than the planar conductor. This result for primary snapover contradicts the analysis of Hastings and Chang that predicts the planar geometry should have a larger snapover voltage than a hemispherical geometry.[6]

The current jump magnitude for the hemisphere was 8 times larger for the primary snapover and 11 times larger for the gas discharge than the same diameter disk conductor. However, the current jump ratio did not show large variations with conductor shape. This suggests that, to a large extent, the current jump increase was not related to snapover or gas discharge dependence on conductor shape directly. Instead it was a result of: (i) overall increased current collection due to the larger collecting surface of the hemisphere, (ii) overall increased current collection due to plasma sheath response to a hemispherical versus planar geometry, and (iii) larger magnitude current jumps which generally accompany delayed snapover and gas discharge onset voltages.

(8 and 9) The Effects of Sample Surface Treatments

To further test the secondary electron model of snapover and to explore methods to inhibit current jumps and stave off the onset of snapover, the insulator surfaces of several samples were treated and tested through repeated cycling. Figure 11 compares typical I-V curves of the treated samples to an untreated ½" Cu-Teflon sample acquired under similar plasma environments and with consistent ramping profiles. Figure 11 also shows optical micrographs of the surfaces.

½" Al-Teflon™ samples were roughened using 70 μm and 100 μm grit sandpaper. By doing so, snapover current jumps were greatly reduced or eliminated. In addition, gas discharge current jumps were typically reduced by more than an order of magnitude. In some cases both snapover and gas discharge current jumps almost completely disappeared. Reduction in snapover is consistent with the fact that roughening can reduce SE collection by recapturing SE's on adjacent surfaces before they can be transported to the conductor or initiate the cascade. However, the observation that both snapover and gas discharge current jumps were suppressed suggest that surface modification had other effects on the processes. Previous experimental studies have reported inconsistent results for roughened surfaces, although Stillwell *et al.* reported similar findings that roughening decreases both snapover and gas discharge collection currents.[7,28]

A ½" Al-Teflon™ sample was coated with a thin film of ~50 μm sized nearly-cubic crystals of MgO suspended in alcohol. The results were very similar to

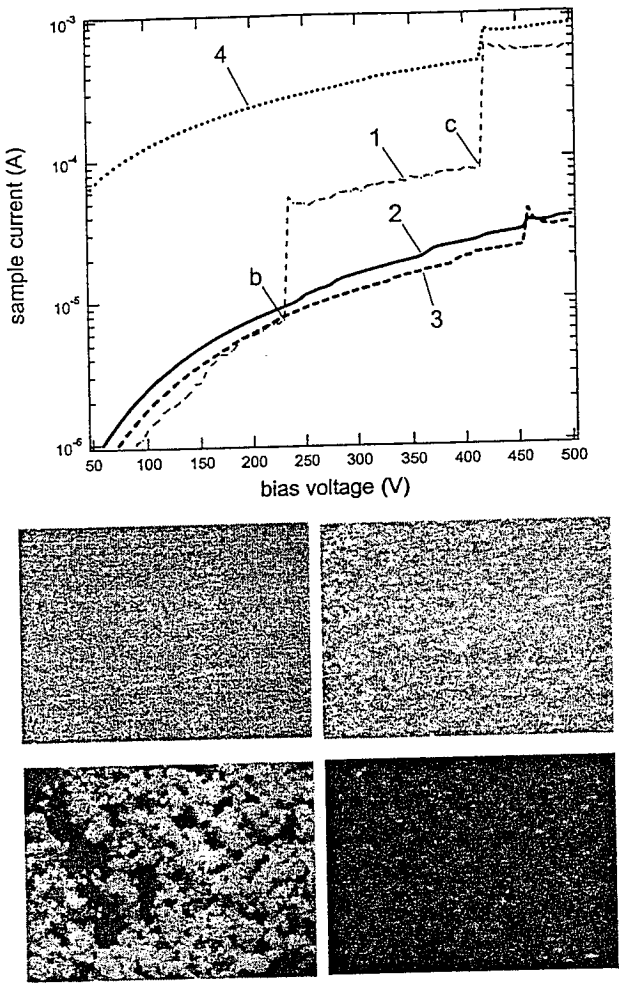

Figure 11. Current-voltage profiles showing the effects of surface modification on the primary snapover (b) and gas discharge (c) current jumps. Profiles shown are for: (1) an untreated ½" Cu-Teflon™ sample (# 2); (2) a ½" Al-Teflon™ sample roughened with 70 μm grit sandpaper; (3) a ½" Al-Teflon™ sample with the dielectric coated with a thin film of ~50 μm sized cubic crystals of MgO; and (4) a ½" Cu-Teflon™ sample with the dielectric coated with a thin film of colloidal microcrystalline graphite (Aerodag™). Optical micrographs of these four samples (in order from left to right) shown below are of ~900 μm x 500 μm areas.

those for roughened surfaces, with snapover nearly fully suppressed and gas discharge current jumps delayed and greatly reduced in magnitude. Since thin film MgO has a maximum SE yield 2 to 8 times that of Teflon™, it is reasonable to expect SE-enhanced current jumps to increase rather than be suppressed. However, the MgO microcrystals can be considered an alternate way to roughen the surface, leading to diminishing effects similar to those described above.

Finally, we applied a thin film of Aerodag™ (colloidal microcrystalline graphite in isopropyl alcohol with a polymer based binder) on 2.3 cm and 4.3 cm OD regions of the dielectric of two ½" Cu-Teflon™ samples. The overall current flow to the conductor was increased by almost two orders of magnitude, while the slope of the I-V curve (*i.e*, the resistance) prior to discharge was reduced. The enhanced collection current resulted from the conducting properties of the graphite. In effect, the conductor size of the samples was increased, resulting in a corresponding increase in the sample collection currents [see *(7a)* above]. Because of the overall current increases, lower voltage snapovers appeared to be suppressed (see Fig. 12). However, closer inspection determined that they were still present with current jump magnitudes similar to those of untreated surfaces. The gas discharge current jump was reduce by a factor of ~2, while the onset voltage remained unchanged. Graphite does not have a first crossover energy; therefore, the SE model predicts a significant decrease in the snapover collection currents. The observed behavior that snapover did occur with current jump magnitudes similar to the untreated Teflon™ sample may have been due to the polymer binder in the Aerodag™ or to the presence of diffusion pump oil contamination.

(10) Optical Spectra of the Gas Discharge Glow

The Paschen discharge current jumps observed were accompanied by an intense blue-violet glow which was captured both on video and by a spectrometer[29,33] to identify the species involved. Spectral measurements of the optical glow performed at voltages between 700 V to 1000 V revealed Argon, but no lines of other species were observed in part due to the low resolution of the spectrometer.[29] Any glow accompanying snapover and gas discharge was too faint to analyze with the spectrometer, although previous studies have reported a faint white glow accompanying snapovers at inception voltages of ~250 V.[4,5] Gas discharge occurring at voltages of 350 V to 600 V was believed to be caused by the out-gassing and subsequent ionization of materials originating from the sample. Further details of the glow discharge are found elsewhere.[29,33]

CONCLUSIONS

In general, more than one current jump was observed over the range of +100 V to 1000 V; these tended to grow in current jump magnitude with higher onset voltages. The current jumps were classified into four major categories based on value of onset voltage, magnitude of current jump, I-V curve behavior, and optical emission as follows: (a) pre-snapover, (b) primary snapover, (c) gas discharge, and (d) Paschen discharge.

Attempts to correlate primary snapover with the SE model of snapover were not successful for a number of reasons:

(i) Snapover inception voltages occurred at much higher

voltages than simple interpretation of the SE model suggests. Primary snapover voltages were > 180 V higher than first crossover energies of either sample dielectrics or diffusion pump oil. Analysis of the ramping rate and plasma/ground offset voltage failed to explain the large discrepancy.

(ii) SE values of the sample dielectric emission characteristics, including the first crossover energy were not known with the necessary accuracy to verify snapover inception voltage dependence on dielectric first crossover energies.

(iii) Snapover onset voltage and current jump magnitude exhibited some dependence on conductor type, which is not expected from the SE model.

(iv) The snapover onset voltage of a hemispherical conductor was higher for a planar conductor of similar material, in contradiction to the prediction of Hastings and Chang based on a SE model.[6] Snapover and gas discharge current jumps showed similar variations between hemispherical and planar conductors.

(v) Estimates of diffusion pump oil deposition rates suggested that the film thickness deposited by chamber contamination was much greater than the maximum escape depth of SE's in diffusion pump oil; this may have obfuscated any snapover dependence on sample dielectric type.

(vi) An inadequate number of samples were tested to conclusively rule out dependence on dielectric first crossover energies.

It was also not obvious whether primary snapover and gas discharge were driven by two completely different mechanisms or were both combination effects of SE emission and ionization of thermal or electron induced desorption of surface materials. Qualitatively, the I-V curves of primary snapover often displayed a hook profile characteristic of gas discharge. In addition, the inception of primary snapover would often drift to higher voltages and increase in current jump magnitude until it was indistinguishable from gas discharge. The hysteresis behavior of primary snapover and gas discharge was similar--the return I-V curve would trace the major current jump back down. Finally, the collection current magnitudes and ratios of both primary snapover and gas discharge were found to follow a power law dependence on conductor diameter with the same exponents within experimental uncertainty. However, snapover current jumps were not as responsive to intermediate voltage Paschen discharge as gas discharge current jumps. This suggested that the gas discharge mechanism was more dependent on surface conditions than was the primary snapover mechanism.

Although the mechanism has not yet been clearly identified by our study, sample surface treatments to the surrounding dielectric were found to suppress snapover. Roughening the surface of the sample dielectric on the order of 50 μm to 100 μm–either by abrasives or by applying a thin layer of MgO–inhibited the collection currents of both snapover and gas discharge. These results suggest possible mitigation strategies for the snapover power loss problem.

ACKNOWLEDGMENTS

The authors gratefully acknowledge the use of the Plasma Interaction Facility at NASA Lewis Research Center and its support staff. This work was partially supported by the NASA Graduate Student Research Program (Davies) and the Rocky Mountain NASA Space Grant Consortium (Thomson and Davies).

REFERENCES

[1] N.J. Stevens, "Interactions Between Spacecraft and the Charged Particle Environment,", Spacecraft Charging Technology-1978, NASA CP-2071, 1979, pp. 268-294.

[2] H. Thiemann, R.W. Schunk, K. Bogus, "Where Do Negatively Biased Solar Arrays Arc?", *Journal of Spacecraft and Rockets*, Vol. 27, No. 5, 1990, pp. 563-565.

[3] G. Hillard and D.C Fergusen, "The SAMPIE Flight Experimental Final Technical Requirements Document," NASA TM-106224, NASA Lewis Res. Center, 1993.

[4] D. Ferguson, G. Hillard, D. Snyder, N. Grier, "The Inception of Snapover on Solar Arrays: A Visualization Technique", Proc. 36th AIAA Aerospace Sciences Meeting and Exhibit, January 12-15, 1998, Reno, Nevada.

[5] NASA Space Environment and Effects Branch http://powerweb.grc.nasa.gov/pvsee/publications/TheBasics.html.

[6] D.E. Hastings, P. Chang, "The Physics of Positively Biased Conductors Surrounded by Dielectrics in Contact with a Plasma", Phys. Fluids B, Vol. 1, No. 5, 1989, pp. 1123-1132.

[7] R.P. Stillwell, R.S. Robison, H.R. Kaufman, "Current Collection from the Space Plasma Through Defects in Solar Array Insulation", *Journal of Spacecraft and Rockets*, Vol. 22, No. 6, 1985, pp. 631-641.

[8] M.R. Carruth Jr., "Plasma Electron Collection Through Biased Slits in a Dielectric", *Journal of Spacecraft and Rockets*, Vol. 24, No. 1, 1987, pp. 79-85.

[9] R.C. Chaky, J.H. Nonnast, J. Enoch, "Numerical Simulation of Sheath Structure and Current-Voltage Characteristics of a Conductor-Dielectric Disk in a Plasma", *Journal of Applied Physics*, Vol. 52, No. 12, 1981, 7092-7098.

[10] R.L. Kessel, R.A. Murray, R. Hetzel, T.P. Armstrong, "Numerical Simulation of Positive-Potential Conductors in the Presence of a Plasma and a Secondary-Emitting Dielectric", *Journal of Applied Physics*, Vol. 57, No. 11, 1985, pp. 4991-4995.

[11] S.T. Brandon, R.L. Kessel, J. Enoch, T.P. Armstrong, "Numerical Simulations of Positively-Biased Probes and Dielectric-Conductor Disks in a Plasma", *Journal of Applied Physics*, Vol. 56, No. 11, 1984, pp. 3215-3222.

[12] M.J. Mandell, I. Katz, G.A. Jongeward, J.C. Roche, "Computer Simulations of Plasma Electron Collection by PIX-II", *Journal of Spacecraft and Rockets*, Vol.23, 1986, pp. 512-518.

[13] H. Thiemann, R.W. Schunk, "Particle-in-Cell Simulations of Sheath Formation Around Biased Interconnectors in a Low-

Earth-Orbit Plasma", *Journal of Spacecraft and Rockets*, Vol. 27, No. 5, 1990, pp. 554-562.

[14] I. Krainsky, W. Lundin, W.L. Gordon, R.W. Hoffmon, *Secondary Electron Emission Yield Annual Report for Period July 1, 1980 to June 30, 1981*, Case Western Reserve University, 1981.

[15] R.F. Willis, D.K. Skinner, "Secondary Electron Emission Yield Behavior of Polymers", *Solid State Communications*, Vol. 13, 1973, pp. 685-688.

[16] C.W. Mueller, "The Secondary Electron Emission of Pyrex Glass", *Journal of Applied Physics*, Vol. 16, 1945, pp. 453-458.

[17] R.E. Chase, W.L. Gordon, R.W. Hoffmon, *Secondary Electron Emission Yield Annual Report for Period July 1, 1978 to June 30, 1979*, Case Western Reserve University, 1979.

[18] S. Thomas, E.B. Pattison, "Range of Electrons and Contributions of Back-Scattered Electrons in Secondary Production in Aluminum", *Journal of Physics D: Applied Physics*, Vol. 3, 1970, pp. 349-357.

[19] H. Bruining, "Secondary Electron Emmision", *Philips Technology Review*, Vol. 13, No. 3, 1938, p. 80.

[20] P. Wargo, B.V. Haxby, W.G. Shepherd, "Preparation and Properties of Thin Film MgO Secondary Emitters", *Journal of Applied Physics*, Vol. 27, No. 11, 1956, pp. 1311-1316.

[21] N. Rey Whetten, A.B. Laponsky, "Secondary Electron Emission from MgO Thin Films", *Journal of Applied Physics*. Vol. 30, No. 3, 1959, pp. 432-435.

[22] K. Goto, K. Ishikawa, "Secondary Electron Emission from Diffusion Pump Oils II.: δ-η Analysis for DC-705", *Japanese Journal of Applied Physics*, Vol. 7, No. 3, 1968, pp. 226-231.

[23] N.T. Grier, "High Voltage Surface-Charged Particles Environment Test Results From Space Flight and Ground Simulation Experiments," NASA TM-79184, 1979.

[24] G.B. Hillard, D.C. Ferguson, "Solar Array Module Plasma Interactions Experiment (SAMPIE): Science and Technology Objectives", *Journal of Spacecraft and Rockets*, Vol. 30, No. 4, 1993, pp. 488-494.

[25] D.C. Ferguson, G.B Hillard, "In-Space Measurement of Electron Current Collection by Space Station Solar Arrays", Proc. 33rd AIAA Aerospace Sciences Meeting and Exhibit, January 9-12, 1995, Reno, Nevada.

[26] B. Vayner, C.V. Doreswamy, D.C. Ferguson, J.T. Galofaro, D.B. Snyder, "Arcing on Aluminum Anodized Plates Immersed in Low Density Plasmas", *Journal of Spacecraft and Rockets*, Vol. 35, No. 6, 1998, pp. 805-811.

[27] R.E. Davies, J.R. Dennison, "Evolution of secondary electron emission characteristics of spacecraft surfaces," Journal of Spacecraft and Rockets, Vol. 34, No. 4, 1997.

[28] A.R. Krauss, "Localized Plasma Sheath Model on Dielectric Discharge of Spacecraft Polymers", *Air Force Weapons Laboratory (AFWL) Final Report*, 1989.

[29] B. Vayner, J. Galofaro, D. Ferguson, W. de Groot, "The Conductor-Dielectric Junction in a Low Density Plasma", Proc. 38th AIAA Aerospace Sciences Meeting and Exhibit, January 10-13, 2000, Reno, Nevada.

[30] W.N. Hansen, Utah State University, private communications, 1999.

[31] W.Y. Chang, J.R. Dennison, Jason Kite and R.E. Davies, "Effects of evolving surface contamination on spacecraft charging," Proc. 38th AIAA Aerospace Sciences Meeting and Exhibit, January 10-13, 2000, Reno, NV.

[32] J.H. Moore, C.C. Davis and M.A. Copeland, *Building Scientific Apparatus*, 2nd Ed. (Addison-Wesley, Reading, MA, 1989), p. 335.

[33] J. Galofaro, B. Vayner, W. de Groot, D. Ferguson, C. Thomson, J.R. Dennison and R.E. Davies, "Inception of snapover and glow induced discharges", Proc. 38th AIAA Aerospace Sciences Meeting and Exhibit, January 10-13, 2000, Reno, NV.